Metal-Catalyzed and Metal-Free Nucleophilic Substitution of 7-I-B$_{18}$H$_{21}$

Kierstyn P. Anderson,[a] Peter I. Djurovich,[b] Victoria P. Rubio,[a] Aimee Liang,[a] and Alexander M. Spokoyny[a]*

[a]Department of Chemistry and Biochemistry and California NanoSystem Institute (CNSI), University of California, Los Angeles, California 90095, USA

[b]Department of Chemistry, University of Southern California, Los Angeles, California 90089, USA

*Corresponding Author Information

E-mail: spokoyny@chem.ucla.edu

ABSTRACT

In this work, two pathways of reactivity are investigated to generate site-specific substitutions at the B7 vertex of the luminescent boron cluster, *anti*-B$_{18}$H$_{22}$. First, a palladium-catalyzed cross-coupling reaction utilizing the precursor 7-I-B$_{18}$H$_{21}$ and a series of model nucleophiles was developed, ultimately producing several B-N and B-O substituted species.

Interestingly, the B-I bond in this cluster can also be substituted in an uncatalyzed fashion, leading to the formation of various B-N, B-O, and B-S products. This work highlights intricate differences corresponding to these two reaction pathways and analyzes the role of solvents and additives on the product distributions. As a result of our synthetic studies, seven new B_{18}-based clusters were synthesized, isolated, and characterized by mass spectrometry and Nuclear Magnetic Resonance (NMR) spectroscopy. The photoluminescent properties of two structurally similar ether and thioether products were further investigated, with both exhibiting blue fluorescence in solution at 298 K and long-lived green or yellow phosphorescence at 77 K. Overall, this work shows for the first time the ability to perform substitution of a boron-halogen bond with nucleophiles in a B_{18}-based cluster, resulting in the formation of photoluminescent molecules.

INTRODUCTION

Boron-halogen (B-X) bond substitution has proven to be a general and versatile transformation that permits precise placement of various substituents on different polyhedral boron cages.[1] This reactivity has led to broad accessibility of new and interesting molecular architectures, particularly for *closo*-boranes such as carboranes and dodecaborate-based clusters.[2] B-X bond substitution in these species is usually achieved through metal-mediated means, such as cross-coupling, that can procure B-C, B-N, B-O, B-P, and B-S bonds.[3] Other methods include light-promoted homolytic cleavage of the boron-halogen bond leading to the formation of a B-centered radical, which can then undergo further substitution reaction.[4] Another strategy for activating a boron-halogen bond centers on the oxidation of the halogen, resulting in the formation of an iodonium substituent that permits a more facile nucleophilic attack at the boron.[5] Interestingly, in contrast to the classical alkyl C-X bonds, nucleophilic substitution of B-X cluster bonds is

generally intractable, with only a handful of reports to date.[6] This can be generally ascribed to the increased strength of B-X bonds and the steric bulk of the cage that prevents nucleophilic attack on the side opposite the halide.[7]

Anti-$B_{18}H_{22}$ is a boron cluster which has gained recent attention as an inherently fluorescent boron hydride (λ_{em} = 410 nm, Φ = 0.97) that has potential for various photoluminescence applications.[8] In order to tune the luminescent properties of the parent compound, selective derivatization methods for this cluster are needed. While there exist a number of routes that can place a halogen moiety onto various vertices of this boron hydride, surprisingly, there have been no reports so far exploring the post-functionalization of these boron-halogen bonds. Unlike *closo*-based clusters for which boron-halogen substitution chemistry has been established, the open-face polyhedral cage configuration of *anti*-$B_{18}H_{22}$ presents several distinct synthetic challenges, including the presence of acidic bridging hydrogens (pK_a = 2.7 and 7.5)[9] and reduced stability profile (Figure 1A).[8h] In this work, we report our initial assessment for the feasibility of substituting a boron-iodine bond at the B7 vertex of the *anti*-$B_{18}H_{22}$ cluster. Specifically, we report the discovery of metal-catalyzed and metal-free pathways capable of producing B-N, B-O, and B-S bonds, ultimately leading to new B_{18}-based chromophores with tunable photoluminescent properties. Overall, this work represents the first example of B-X bond substitution in *anti*-$B_{18}H_{22}$ and provides a potential roadmap toward the development of a broad scope of B_{18}-based luminescent materials.

RESULTS AND DISCUSSION

To examine the feasibility of metal-catalyzed cross-coupling for halogenated *anti*-$B_{18}H_{22}$ clusters, we decided to employ the Buchwald-Hartwig amidation conditions previously reported

for B-iodo-carboranes.[10] Monoiodinated $7\text{-}I\text{-}B_{18}H_{21}$ (**1**) was selected as the borane precursor due to its straightforward and high-yielding synthesis[8c] and 2,2,2-trifluoroacetamide (**I**) was used as a coupling partner. This nucleophile was specifically chosen for its inability to undergo β-hydride elimination and its low pK_a resulting in facile deprotonation during the transmetallation step.[11] The reaction progress and products formed were monitored *in situ* by electrospray ionization mass spectrometry in the negative mode (ESI(-)MS). While the initially selected conditions did not result in significant conversion of the starting material as observed by ESI(-)MS (Figure 1C, Entry 1), a mass consistent with product **2** was observed when the ligand and catalyst loading were increased from 10 mol% and 5 mol% to 50 mol% and 25 mol%, respectively (Figure 1C, Entry 2). However, degradation to a non-cluster species was also indicated by a significant amount of a water-soluble solid that manifested as a sharp singlet at ~13 ppm in the ^{11}B NMR spectrum. The formation of this unidentified byproduct was observed to a lesser extent when 1,4-dioxane was used as a solvent, however only $B_{18}H_{22}$ was observed by ESI(-)MS, suggesting a competing reduction pathway (Figure 1C, Entry 3). We previously employed palladium-based precatalysts in combination with biaryl phosphine ligands, which proved superior in cross-coupling efficiency for B-halo-carboranes compared to the conventional Pd_2dba_3 (tris(dibenzylideneacetone)dipalladium(0)) precursor (Figure 1B).[12] Improved conversion to product **2** in 1,4-dioxane was thereby achieved with a RuPhos/RuPhos Pd G4 precatalyst system (L2/[L2Pd], Figure 1B). Further optimization revealed that L2/[L2Pd] loading could be reduced to 25 mol%/10 mol% while maintaining nearly complete conversion (Figure 1C, Entry 4). With these optimized conditions we were able to purify the product mixture and isolate **2** as an analytically pure solid in 24% yield. The significant yield reduction is attributed to both the competing reduction pathway that produces $B_{18}H_{22}$ and the acidified silica gel column

chromatography conditions, which results in loss of the product material.[6c,13] Nevertheless, the reaction conditions also proved effective with a K^{t}BuO substrate (**II**) to yield the monosubstituted boron cluster product, **3** (Figure 1C, Entry 5). This B-O cross-coupling can also be conducted in a microwave reactor at 100°C for 45 minutes (Figure 1C, Entry 6). In addition to appending the alkyl ^{t}BuO substituent, we found that this reaction is suitable for the bulky aromatic substrate potassium 2,6-dimethylphenolate to yield **4**. The metal-mediated nature of these reactions is supported by Figure S46.
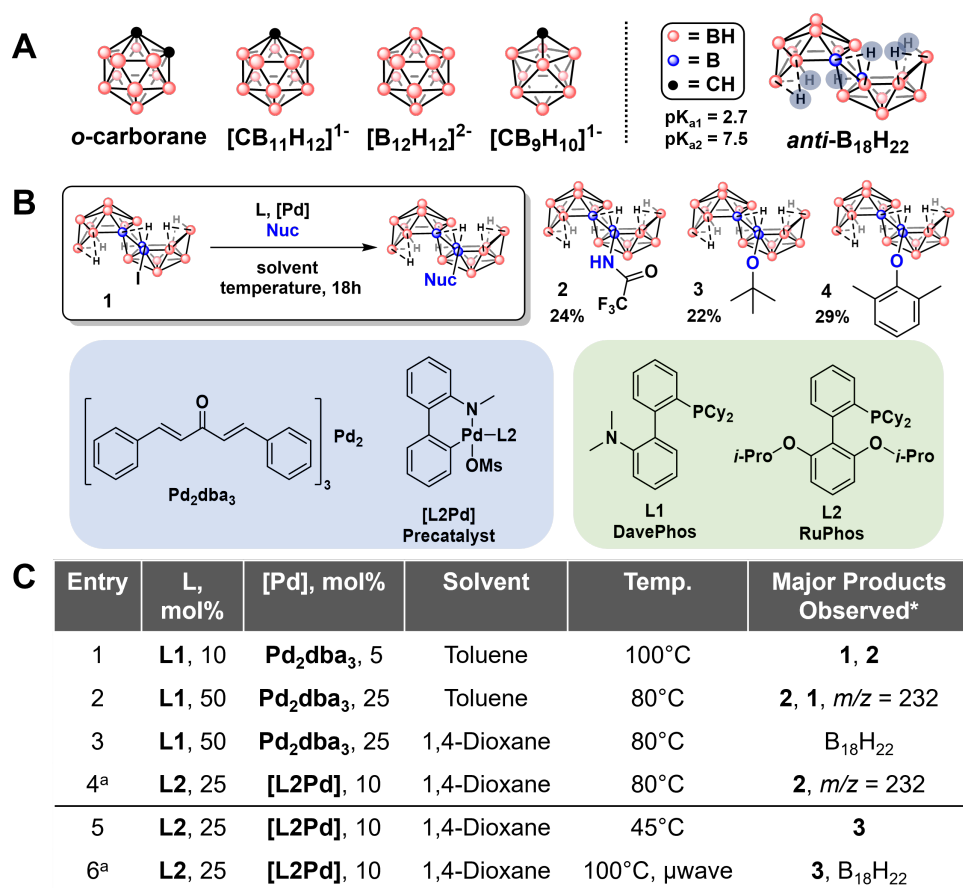
Figure 1. A) Select *closo*-boranes that can undergo metal-catalyzed cross-coupling vs. the *nido anti*-B$_{18}$H$_{22}$ cluster. B) General cross-coupling conditions, ligands and catalysts used, and resulting products **2-4** with isolated yields. C) Screening conditions employed to produce products **2** and **3**. See SI for general screening conditions procedure. [a]Done on a 30mg scale. *In order of decreasing intensity by ESI(-)MS.

With the isolated B-N and B-O products in hand, we turned to heteronuclear NMR spectroscopy for further characterization of compounds **2-4**; each were subject to ^{13}C, $^{1}H\{^{11}B\}$, ^{11}B NMR and $^{1}H\{^{11}B\}$-$^{11}B\{^{1}H\}$ Heteronuclear Multiple Quantum Coherence (HMQC) analysis (Figures S8-12). Taking **3** as an example, the presence of the *tert*-butyl group is supported by characteristic resonances in the ^{13}C NMR spectrum (-29.95 ppm and-78.24 ppm) and the singlet at 1.48 ppm in the $^{1}H\{^{11}B\}$ NMR spectrum. Also present in the $^{1}H\{^{11}B\}$ NMR spectrum are resonances corresponding to the 15 terminal and 6 bridging hydrogen nuclei on the boron cage, which is consistent with a monosubstituted product. The 18 boron nuclei are represented in the $^{11}B\{^{1}H\}$ NMR spectrum, and analysis of the corresponding ^{11}B NMR spectrum shows that all but three of these resonances exhibit doublet splitting, indicating they are bound to a terminal hydrogen. The three singlets at 8.33, 0.71, and -1.10 ppm should correspond to vertices B5, B6, and the newly substituted B7 (see Figure 2 for the numbering scheme). Integration of the boron resonances indicate that while 18 boron nuclei are present, several share similar chemical shifts, which makes definitive assignment of the boron resonances between 5 and -5 ppm more challenging. Therefore, a HMQC study of the $^{11}B\{^{1}H\}$ and $^{1}H\{^{11}B\}$ NMR spectra was conducted to assign the boron resonances and to confirm the overall structure of the molecule (Figure 2). The bridging hydrogen resonances in the HMQC spectrum provide an ideal starting point for the analysis of the 2D spectrum because they correspond to two separate boron nuclei. For example, the identification of the B8-B9 bridging hydrogen H8-9 resonance at -2.90 ppm[10c] leads to the assignment of the resonances at -3.08 ppm and 2.62 ppm to the boron nuclei B8 and B9, respectively. In addition, the B9 resonance corresponds to a proton resonance at -0.26 ppm, which then correlates to two different boron resonances. This must signify the B9-B10 bridging hydrogen, which in turn leads to the assignment of the resonance at 9.63 ppm to the B10 nucleus. Continuing this process leads
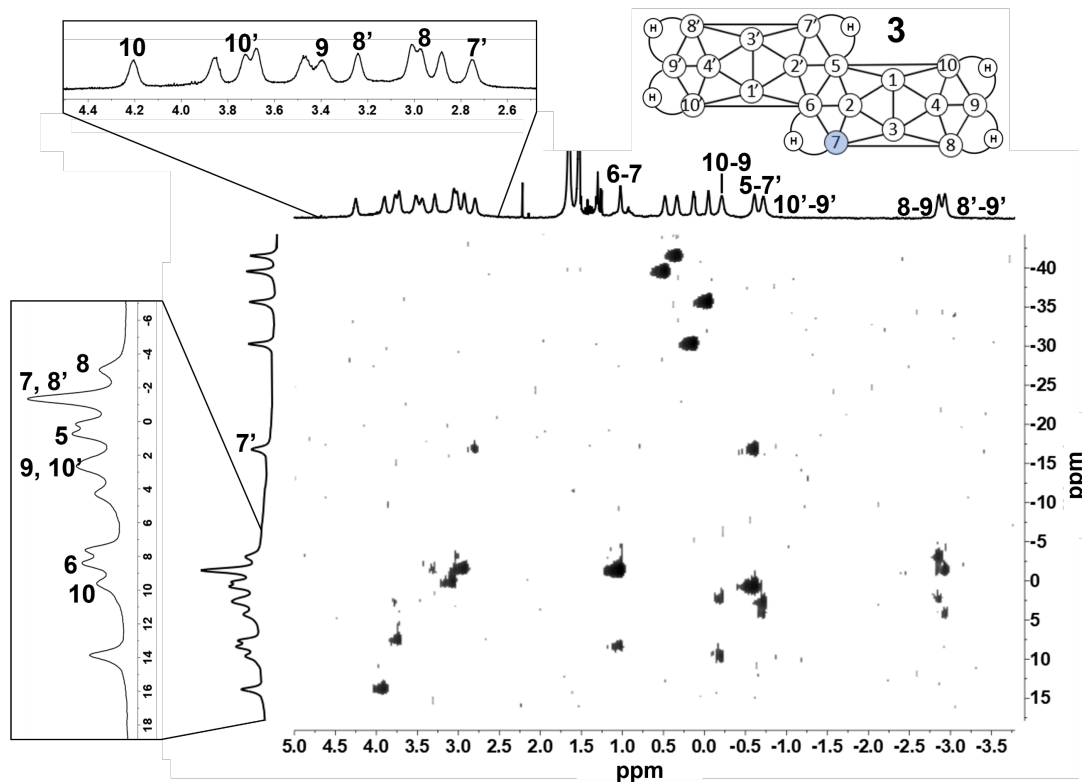
Figure 2. $^1H\{^{11}B\}$-$^{11}B\{^1H\}$ HMQC of **3** with select boron and hydrogen resonances labeled according to the numbering scheme at the top (substituted B7 vertex is highlighted in blue).

to the identification of the bridging hydrogens H5-7' and H6-7 *via* their resonances at -0.66 and 0.98 ppm, respectively. From this, one can assign the B5 (0.71 ppm), B6 (8.33 ppm), and B7 (-1.10 ppm) nuclei to the initially observed singlets in the ^{11}B NMR spectrum. The significant downfield shift of the B7 resonance compared to the B7' resonance and the absence of a B7 terminal hydrogen resonance is consistent with the B7-substituted nature of the cluster.

As we turned our attention to expanding the scope of cross-coupling to forge B-S bonds, we noticed product masses in the ESI(-)MS of the crude reaction mixtures that were not observed in previous reactions. For example, when the cross-coupling conditions were applied to potassium 2,6-dimethylthiophenolate (**III**), a mass corresponding to the desired B-S substituted cluster product plus a dioxane solvent molecule (*m/z* = 440.38) was the major species by ESI(-)MS.

Similar results were observed when the reaction was conducted in THF (m/z = 424.38) (Figure S19). Upon isolation of this THF-containing compound, analysis by 1D and 2D ^{11}B NMR spectroscopy indicated a monosubstituted cluster pattern, with the functionalized B7 resonance at -3.83 ppm. The ^{1}H{^{11}B} NMR spectrum contained resonances corresponding to 21 cluster hydrogens (-3 to 5 ppm) and the thioether group (7.11 and 2.57 ppm), but the distinctive THF resonances at 1.85 and 3.76 ppm were not observed. Instead, triplets at 3.97 and 2.73 ppm and multiplets at 1.82 and 1.71 ppm were present, suggesting the presence of a linear alkyl ether motif rather than an intact ethereal ring (Figure S20). This observation was further supported by ^{13}C and ^{13}C APT NMR spectroscopic experiments (Figures S23-25), which depict carbon resonances for both the thioether (143.20, 133.78, 128.25, 128.23, 22.8 ppm) and alkyl ether (70.33, 35.21, 30.49, and 36.56 ppm). In total, these data led us to conclude that the compound consisted of a B7-O bound, ring-opened THF molecule that resides between the electrophilic boron cluster and nucleophilic substrate (**5**).

To our surprise, further control experiments that excluded the palladium-based precatalyst and ligand from the reaction led to significant formation of **5** when the mixture was analyzed by ESI(-)MS *in situ*. This observation ultimately suggested that nucleophilic substitution of 7-I-B$_{18}$H$_{21}$ can potentially proceed *via* a separate mechanism that does not involve oxidative addition of Pd(0) into a B-I bond. This is significant considering that a metal-free route toward B$_{18}$H$_{22}$ functionalization could alleviate some of the limitations observed in the metal-catalyzed reactions, specifically the competing reduction process that produces B$_{18}$H$_{22}$ and the slow reductive elimination step that necessitates sterically bulky substrates.[16] To explore this opportunity further, we examined the conditions under which products similar to **5** could form for various substrates (Figure 3A). When individual substrates **I-V** were combined with **1** in THF at 80-100°C, the ESI(-

)MS spectrum of each reaction mixture exhibited only the mass corresponding to its respective alkyl ether product derived from THF ring-opening. The only exception was the K*t*BuO (**II**) reaction mixture, which also contained a mass corresponding to the direct nucleophilic substitution product **3**. To determine if interconversion between these two compounds was possible, the reaction mixture was further refluxed for 18 hours but showed no change in the product distribution as observed by ESI(-)MS. This finding led us to consider two possible pathways of reactivity for this reaction (Figure 3B). The Lewis acidic B_{18}-based cluster can interact with THF[10h] to weaken the B-I bond, providing sufficiently nucleophilic substrates such as **II** the opportunity to attack the boron atom (Figure 3B(a)). Weaker nucleophiles, however, will react at the THF carbon to yield the ring-opened product (Figure 3B(b)). To probe the conditions under which each pathway could be potentially favored, we reacted **1** with **II** in THF at room temperature. This provided nearly full conversion to **3** as observed by ESI(-)MS, suggesting that the ring-opened product is favored at
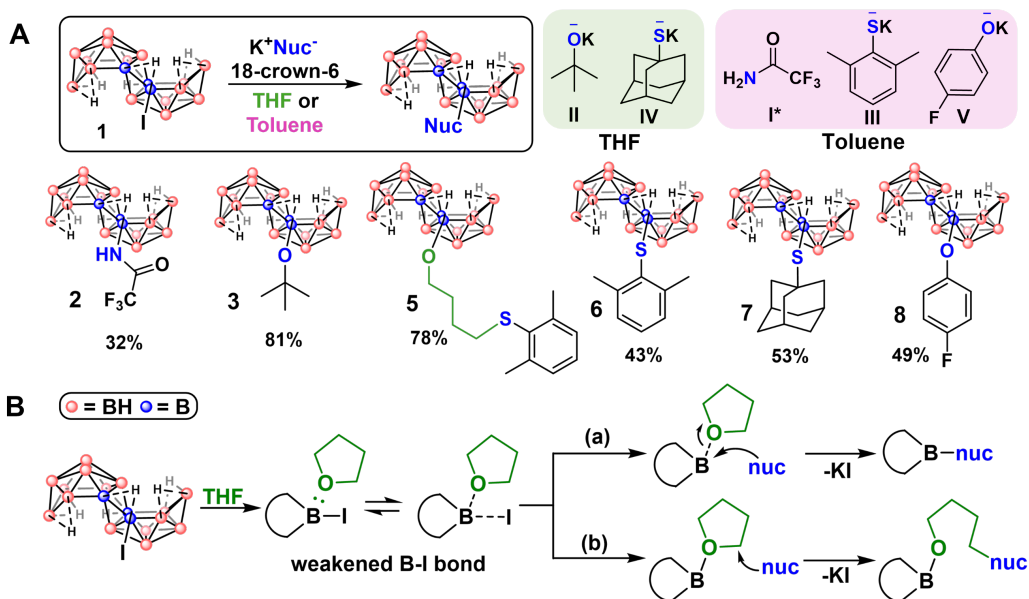
Figure 3. A) Reaction for nucleophilic substitution, substrates employed, and resulting products. Substrates can undergo substitution in THF (green) or toluene (pink). B) Pathways of reactivity for nucleophiles reacting with **1** in THF solution. *K_3PO_4 is included in the reaction mixture.

elevated temperatures. These results, however, were exclusive to **3**; only the THF-derived products were observed by ESI(-)MS for the other substrates, even when the reactions were conducted at -78°C. While sulfur-based reagents **III** and **IV** are more nucleophilic than their oxygen counterparts, the thermodynamic preference for B-O bond formation compared to B-S congener renders the formation of products **6** and **7** less favorable than the corresponding THF-derived products.[17] In an effort to overcome this, we found that incorporation of 18-crown-6 in the reaction mixture increases conversion to products **3** and **7** as observed by ESI(-) MS, possibly due to the increased Lewis basicity of the substrate caused by sequestration of the cation.[17] The remaining substrates **I**, **III**, and **V** however, still required a more inert solvent to avoid the ring-opening pathway altogether (Figure 3A, pink). As such, when **I**, **III**, and **V** are reacted with **1** in toluene there is no conversion observed by ESI(-)MS, yet including 18-crown-6 in the reaction mixture ultimately produces the desired compounds **2**, **6**, and **8**. Overall, the ability for substrates **I**, **III** and **V** to undergo nucleophilic substitution is aided not only by the crown ether but also toluene, which has a destabilizing effect on the nucleophile by solvating it to a lesser degree than THF.[18] Compounds **2**, **3**, and **5-8** can be easily isolated from the corresponding reaction mixtures. Structural formulations of these products were confirmed by ESI(-)MS and ^{1}H{^{11}B}, ^{11}B{^{1}H}, ^{11}B, ^{13}C, ^{19}F, HMQC NMR spectroscopy. Interestingly, neither the reactions in THF nor toluene led to significant formation of **4**, potentially due to its weak nucleophilicity. Cross-coupling therefore remains the most viable route for producing **4** and other structures unsuitable for nucleophilic substitution. Still, the ability for 7-I-$B_{18}H_{21}$ to undergo metal-free nucleophilic substitution at the B-I bond is remarkable given the comparatively inert nature of boron-halogen bonds in other polyhedral borane clusters.

Given that this is the first report of ether and thioether-functionalized *anti*-$B_{18}H_{22}$, we wanted to benchmark the luminescent properties of these new derivatives. Specifically, the structurally similar compounds **4** and **6** were assessed to gauge the effects of oxygen vs. sulfur on cluster luminescence (Figure 4). In cyclohexane solution, the absorption of both compounds is largely in the UV region, with (ε_{346} = 6600 $M^{-1}cm^{-1}$ for **4** and ε_{392} = 3300 $M^{-1}cm^{-1}$ for **6**). Emission spectra of these solutions show blue fluorescence at 427 nm and 460 nm in **4** and **6**, respectively (Figure 4, S50, S52). Notably, this emission was exceptionally weak, with quantum yields (Φ) less than 0.01. However, when the measurements were repeated at 77 K in methylcyclohexane the luminescence was significantly shifted to the red (λ_{em} = 530 nm for **4** and λ_{em} = 572 nm for **6**). The measured emission lifetimes (τ) at these wavelengths show long-lived, phosphorescent processes, with τ = 360 ms for **4** and τ = 7.7 ms for **6**. (Figures S51, S53). Phosphorescence is typically seen in molecules containing heavy atoms, which lend the molecule spin-orbit coupling (SOC) needed to increase the efficiency of intersystem crossing (ISC) from the singlet excited state to the triplet excited state. Based on the weak fluorescence in these two compounds, it appears that SOC arising from oxygen and sulfur leads to efficient ISC. This phenomenon is consistent with TD-DFT calculations of **4** and **6**, in which the valence orbitals participating in lowest electronic transitions (Figures S54-55) support El-Sayed's rules for efficient ISC.[19] The extraordinarily long phosphorescent lifetimes in **4** and **6** provide ample opportunity for competitive non-radiative decay to occur (e.g., through molecular motion), ultimately resulting in minimal luminescence at ambient conditions. At 77 K, however, the molecules are constrained in a frozen matrix that inhibits these non-radiative decay processes and thus permits strong phosphorescence. This data highlights the varying effects that substituents can have on the photophysical properties
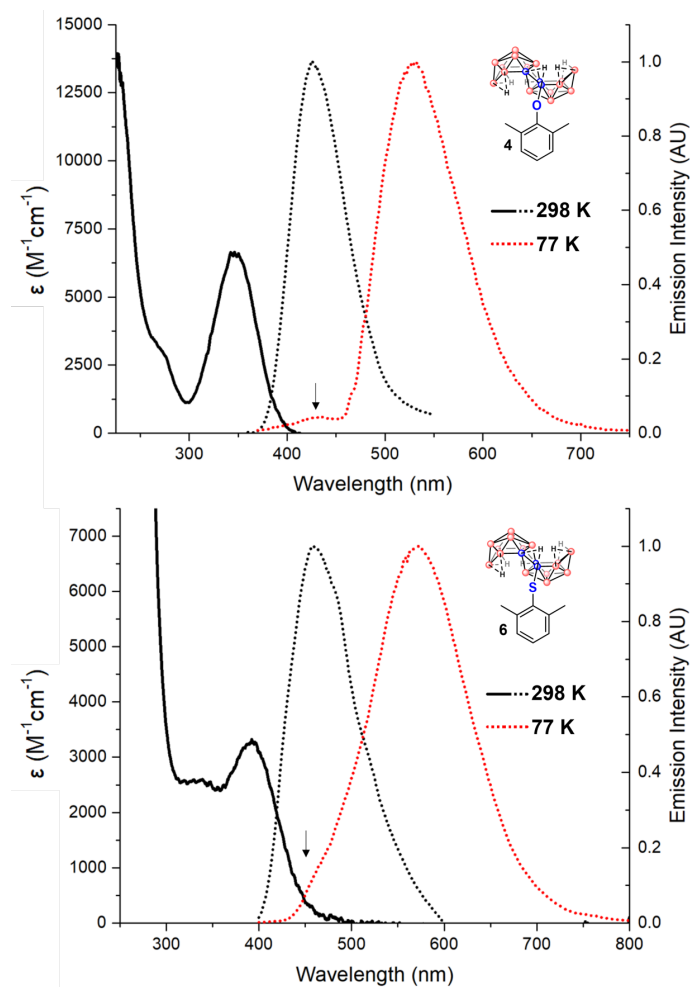
Figure 4. Absorption (solid line) and emission (dotted line) spectra of compounds **4** (top) and **6** (bottom). Emission spectra at 298 K and 77 K display fluorescence and phosphorescence, respectively. The arrows indicate fluorescent shoulders visible in the 77 K spectra. For **4**, λ_{exc} = 340 nm at 298 K, λ_{exc} = 350 nm at 77 K. For **6**, λ_{exc} = 380 nm.

of *anti*-$B_{18}H_{22}$ and shows that B-O and B-S connectivity alters the absorption, emission, and fluorescent behavior of the corresponding B_{18}-based cluster.

In this work we detail two new and complementary strategies for generating nitrogen, oxygen, and sulfur-functionalized *anti*-$B_{18}H_{22}$ analogues from 7-I-$B_{18}H_{21}$. We first demonstrate that palladium-catalyzed cross-coupling can forge B-N and B-O bonds at the B7 vertex with

sterically hindered substrates. To our surprise, we discovered that these connectivities could be produced through a metal-free nucleophilic substitution pathway, which also proved applicable for generating B-S functionalized clusters. In addition to unveiling this unique reactivity of monoiodinated $B_{18}H_{22}$, we demonstrate that the luminescence of the parent borane can be modulated through cage functionalization. Aside from a rare example of a metal-free nucleophilic substitution chemistry of a boron-halogen moiety in a boron cluster, this work broadens the scope of luminescent boron cluster-based molecules.[18]

ASSOCIATED CONTENT

Supporting Information.

The Supporting Information is available free of charge. Detailed experimental and analytical procedures, characterization data, and DFT calculations (PDF)

AUTHOR INFORMATION

Corresponding Author

Alexander M. Spokoyny – *Department of Chemistry and Biochemistry, University of California, Los Angeles, Los Angeles, California 90095, United States; California NanoSystems Institute, University of California, Los Angeles, Los Angeles, California 90095, United States*; https://orcid.org/ 0000-0002-5683-6240; Email: spokoyny@chem.ucla.edu

Kierstyn P. Anderson – *Department of Chemistry and Biochemistry, University of California, Los Angeles, Los Angeles, California 90095, United States;* https://orcid.org/0000-0002-0297-0727

Peter I. Djurovich – *Department of Chemistry, University of Southern California, Los Angeles, California 90089, United States;* https://orcid.org/0000-0001-6716-389X

Victoria P. Rubio – *Department of Chemistry and Biochemistry, University of California, Los Angeles, Los Angeles, California 90095, United States*

Aimee Liang – *Department of Chemistry and Biochemistry, University of California, Los Angeles, Los Angeles, California 90095, United States*

Author Contributions

The manuscript was written through contributions of all authors. All authors have given approval to the final version of the manuscript.

REFERENCES

1. (a) Grimes, R.N. *Carboranes, 3rd ed*. Academic Press, 2016. (b) Lipscomb, W.N. *Boron Hydrides*. Courier Corporation, 2013.

2. Recent reviews: (a) Fisher, S.P.; Tomich, A.W.; Lovera, S.O.; Kleinsasser, J.F.; Guo, J.; Asay, M.J.; Nelson, H.M.; LaVallo, V. Nonclassical Applications of *closo*-Carborane Anions: From Main Group Chemistry and Catalysis to Energy Storage. *Chem. Rev.* 2019, *119*, 8262-8290. (b) Dash, B.P.; Satapathy, R.; Maguire, J.A.; Hosmane, N.S. Polyhedral boron clusters in materials science. *New J. Chem.* 2011, *35*, 1955-1972. Núñez, R.; Tarrés, M.; Ferrer-Ugalde. A.; de Biani,

F.F.; Teixidor, F. Electrochemistry and Photoluminescence of Icosahedral Carboranes, Boranes, Metallacarboranes, and Their Derivatives. *Chem. Rev.* **2016**, *116*, 14307-14378.

3.   Recent reviews: (a) Dziedzic, R.M. and Spokoyny, A.M. Metal-catalyzed cross-coupling chemistry with polyhedral boranes. *Chem. Commun.* 2019, *55*, 430-442. (b) Olid, D.; Núñez, R.; Viñas, C.; Teixidor, F. Method to produce B-C, B-P, B-N and B-S bonds in boron clusters. *Chem. Soc. Rev.* 2013, *42*, 3318-3336.

4. Key select examples: (a) Trofimenko, S. Photoinduced Nucleophilic Substitution in Halogenated Clovoboranes. *J. Am. Chem. Soc.* 1966, *88*, 1899-1904. (b) Li, S. and Xie, Z. Visible-Light-Promoted Nickel-Catalyzed Cross-Coupling of Iodocarboranes with (Hetero)Arenes via Boron-Centered Carboranyl Radicals. *J. Am. Chem. Soc.* **2022**, *144*, 7960-7965.

5. Key select examples: (a) Marshall, W.J.; Young, R.J.; Grushin, V.V. Mechanistic Features of Boron-Iodine Bond Activation of B-Iodocarboranes. *Organometallics* **2001**, *20*, 523-533. (b) Kaszyński, P. and Ringstrand, B. Functionalization of *closo*-Borates via Iodonium Zwitterions. *Angew. Chem. Int. Ed.* **2015**, *54*, 6576-6581. (c) Zhu, T.-C.; Xing, Y.-Y.; Sun, Y.; Duttwyler, S.; Hong, X. Directed B-H functionalization of the *closo*-dodecaborate cluster *via* concerted iodination-deprotonation: reaction mechanism and origins of regioselectivity. *Org. Chem. Front.* **2020**, *7*, 3648-3655.

6.   Key select examples: (a) Buades, A.B.; Arderiu, V.S.; Olid-Britos, D.; Viñas, C.; Sillanpää, R.; Haukka, M.; Fontrodona, X.; Paradinas, M.; Ocal, C.; Teixidor, F. Electron Accumulative Molecules. *J. Am. Chem. Soc.* **2018**, *140*, 2957-2970. (b) Stogniy, M. Y.; Anufriev, S.A.; Shmal'ko, A.V.; Antropov, S.M.; Anisimov, A.A.; Suponitsky, K.Y.; Filippov, A.O.; Sivaev, I.B. The unexpected reactivity of 9-iodo-*nido*-carborane: from nucleophilic substitution reactions to the

synthesis of tricobalt tris(dicarbollide) Na[4,4',4"-(MeOCH$_2$CH$_2$O)$_3$-3,3',3"-Co$_3$(μ^3-S)(1,2-C$_2$B$_9$H$_{10}$)$_3$]. *Dalton Trans*. **2021**, *50*, 2671-2688. (c) Ewing, W. C.; Carroll, P.J.; Sneddon, L.G. Syntheses and Surprising Regioselectivity of 5- and 6-Substituted Decaboranyl Ethers via the Nucleophilic Attack of Alcohols on 6- and 5-Halodecaboranes. *Inorg. Chem.* **2011**, *50*, 4054-4064. (d) Wright, J. H.; Kefalidis, C.E.; Tham, F.S.; Maron, L.; Lavallo, V. Click-like Reactions with the Inert HCB$_{11}$Cl$_{11}^-$ Anion Lead to Carborane-Fused Heterocycles with Unusual Aromatic Character. *Inorg. Chem.* **2013**, *52*, 6223-6229. (b) Finze, M.; Sprenger, J.A.P.; Schaack, B.B. Salts of the 1-cyanocarba-*closo*-dodecaborate anions [1-NC-*closo*-1-CB$_{11}$X$_{11}$]$^-$ (X = H, F, Cl, Br, I). *Dalton Trans*. **2010**, *39*, 2708-2716.

7.   (a) Zakharkin, L. N. and Kalinin, V. N. Action of nucleophilic reagents on B-halocarboranes. *BACCA* **1971**, *20*, 2185-2187. (b) Winberg, K.J.; Mume, E.; Tolmachev, V.; Sjöberg, S. Radiobromination of *closo*-carboranes using palladium-catalyzed halogen exchange. *J. Label. Compd. Radiopharm.* **2005**, *48*, 195-202.

8.   (a) Pitochelli, A. R. and Hawthorne, M.F. The Preparation of a New Boron Hydride B$_{18}$H$_{22}$. *J. Am. Chem. Soc.* **1962**, *84*, 3218. (b) Cerdán, L.; Braborec, J.; Garcia-Moreno, I.; Costela, A.; Londesborough, M.G.S. A borane laser. *Nature Commun.* **2015**, *6*, 5958. (c) Londesborough, M. G. S.; Dolanský, J.; Bould, J.; Braborec, J.; Kirakci, K.; Lang, K.; Císařová, I.; Kubát, P.; Roca-Sanjuán, D.; Francés-Monerris, A.; Slušná, L.; Noskovičová, E.; Lorenc, D. Effect of Iodination on the Photophysics of the Laser Borane *anti*-B$_{18}$H$_{22}$: Generation of Efficient Photosensitizers of Oxygen. *Inorg. Chem.* **2019**, *58*, 10248-10259. (d) Anderson, K.P.; Waddington, M.A.; Balaich, G.J.; Stauber, J.M.; Bernier, N.A.; Caram, J.R.; Djurovich, P.I.; Spokoyny, A.M. A molecular boron cluster-base chromophore with dual emission. *Dalton Trans*. **2020**, *49*, 16245-16251. (e) Londesborough, M. G. S.; Dolanský, J.; Jelínek, T.; Kennedy, J.D.; Císařová, I.; Kennedy, R.D.;

Roca-Sanjuán, D.; Francés-Monerris, A.; Lang. K.; Clegg, W. Substitution of the laser borane *anti*-$B_{18}H_{22}$ with pyridine: a structural and photophysical study of some unusually structured macropolyhedral boron hydrides. *Dalton Trans*. **2018**, *47*, 1709-1725. (f) Chen, J.; Xiong, L.; Zhang, L.; Huang, X.; Meng, H.; Tan, C. Synthesis, aggregation-induced emission of a new *anti*-$B_{18}H_{22}$-isoquinoline hybrid. *Chem. Phys. Lett*. **2020**, *747*, 137328. (g) Saurí, V.; Oliva, J.M.;0 Hnyk, D.; Bould, J.; Braborec, J.; Merchán, M.; Kubát, P.; Císařová, I.; Lang, K.; Londesborough, M.G.S. Tuning the Photophysical Properties of *anti*-$B_{18}H_{22}$: Efficient Intersystem Crossing between Excited Singlet and Triplet States in New 4,4'-$(HS)_2$-*anti*-$B_{18}H_{20}$. *Inorg. Chem*. **2013**, *52*, 9266-9274. (h) Anderson, K.P.; Hua, A.S.; Plumley, J.B.; Ready, A.D.; Rheingold, A.L.; Peng, T.L.; Djurovich, P.I.; Kerestes, C.; Snyder, N.A.; Andrews, A.; Caram, J.R.; Spokoyny, A.M. Benchmarking the dynamic and luminescent properties and UV stability of $B_{18}H_{22}$-based materials. *Dalton Trans*. **2020**. Article ASAP. DOI: 10.1039/D2DT01225A.

9.   (a) Stanko, V. I.;Chapovskii, Y.A.; Brattsev, V.A.; Zakharkin, L.I. The Chemistry of Decaborane and its Derivatives. *Russ. Chem. Rev*. **1965**, *34*, 424-439. (b) G. A. Guter and G. W. Schaeffer, The Strong Acid Behavior of Decaborane. *J. Am. Chem. Soc*. **1956**, *78*, 3546. (c) King, R.B. Defective Vertices in *closo*- and *nido*-Borane Polyhedra. *Inorg. Chem*. **2001**, *40*, 6369-6374. (d) Simpson, P.G. and Lipscomb, W.N. Molecular, Crystal, and Valence Structures of $B_{18}H_{22}$. *J. Chem. Phys*. **1963**, *39*, 26-34. (e) Olsen, F.P.; Vasavada, R.C.; Hawthorne, M.F. The chemistry of n-$B_{18}H_{22}$ and i-$B_{18}H_{22}$. *J. Am. Chem. Soc*. **1968**, *90*, 3946-3951.

10. Sevryugina, Y.; Julius, R.L.; Hawthorne, M.F. Novel Approach to Aminocarboranes by Mild Amidation of Selected Iodo-carboranes. *Inorg. Chem*. **2010**, *49*, 10627-10634.

11.   (a) Bagno, A. and Comuzzi, C. Deprotonation of Amides and Polyfunctional Imides Probed by Heteronuclear NMR and Quantum Chemical Calculations. *Eur. J. Org. Chem.* **1999**, 287-295. (b) Reis, O.; Koyuncu, H.; Esiringu, I.; Sahin, Y.; Gulcan, O. A new method for the synthesis of rasagiline. European Patent EP2663545B1, January 13, 2011.

12.   (a) Dziedzic, R.M.; Saleh, L.M.A.; Axtell, J.C.; Martin, J.L.; Stevens, S.L.; Royappa, A.T.; Rheingold, A.L.; Spokoyny, A.M. B-N, B-O, and B-CN Bond Formation via Palladium-Catalyzed Cross-Coupling of B-Bromo-Carboranes. *J. Am. Chem. Soc.* **2016**, *138*, 9081-9084. (b) Dziedzic, R.M.; Martin, J.L.; Axtell, J.C.; Saleh, L.M.A.; Ong, T.-C.; Yang, Y.-F.; Messina, M.S.; Rheingold, A.L.; Houk, K.N.; Spokoyny, A.M. Cage-Walking: Vertex Differentiation by Palladium-Catalyzed Isomerization of B(9)-Bromo-*meta*-Carborane. *J. Am. Chem. Soc.* **2017**, *139*, 7729-7732. (c) Mu, X.; Hopp, M.; Dziedzic, R.M.; Waddington, M.A.; Rheingold, A.L.; Sletten, E.M.; Axtell, J.C.; Spokoyny, A.M. Expanding the Scope of Palladium-Catalyzed B-N Cross-Coupling Chemistry in Carboranes. *Organometallics*, **2020**, *39*, 4380-4386. (d) Kataki-Anastasakou, A.; Axtell, J.C.; Hernandez, S.; Dziedzic, R.M.; Balaich, G.J.; Rheingold, A.L.; Spokoyny, A.M.; Sletten, E.M. Carboranes Guests for Cucurbit[7]uril Facilitate Strong Binding and On-Demand Removal. *J. Am. Chem. Soc.* **2020**, *142*, 20513-20518. (e) Dziedzic, R.M.; Axtell, J.C.; Rheingold, A.L.; Spokoyny, A.M. Off-Cycle Processes in Pd-Catalyzed Cross-Coupling of Carboranes. *Org. Process Res. Dev.* **2019**, *23*, 1638-1645. (f) Biscoe, M.R.; Fors, B.P.; Buchwald, S.L. A New Class of Easily Activated Palladium Precatalysts for Facile C-N Cross-Coupling Reactions and the Low Temperature Oxidative Addition of Aryl Chlorides. *J. Am. Chem. Soc.* **2008**, *130*, 6686-6687. (g) Bruno, N.C.; Tudge, M.T.; Buchwald, S.L. Design and preparation of new palladium precatalysts for C-C and C-N cross-coupling reactions. *Chem. Sci.* **2013**, *4*, 916-920. (h) Bruno, N.C. and Buchwald, S.L. Synthesis and Application of Palladium Precatalysts that

Accommodate Extremely Bulky Di-*tert*-butylphosphino Biaryl Ligands. *Org. Let.*. **2013**, *15*, 2876-2879. (i) Bruno, N.C.; Niljianskul, N.; Buchwald, S.L. *N*-substituted 2-Aminobiphenylpalladium Methanesulfonate Precatalysts and Their Use in C-C and C-N Cross-Couplings. *J. Org. Chem.* **2014**, *79*, 4161-4166.

13.   Loffredo, R. E.; Drullinger, L.F.; Slater, J.A.; Turner, C.A.; Norman, A.D. Preparation and properties of 6-ethoxy-, 6-phenyl-, and 6-trimethylsiloxydecaborane(14). *Inorg. Chem.* **1976**, *15*, 478-480.

14.   Tian, J.; Wang, G.; Qi, Z.-H.; Ma, J. Ligand Effects of BrettPhos and RuPhos on Rate-Limiting Steps in Buchwald-Hartwig Amination Reaction Due to the Modulation of Steric Hindrance and Electronic Structure. *ACS Omega*, **2020**, *5*, 21385-21391.

15.   Finch, A.; Gardner, P.J.; Watts, G.B. Thermochemistry of the trialkylthioboranes and triphenylthioborane. *J. Chem. Soc. Faraday Trans.* **1967**, *63*, 1603-1607.

16.   Hamlin, T.A.; Swart, M.; Bickelhaupt, F.M. Nucleophilic Substitution (S_N2): Dependence on Nucleophile, Leaving Group, Central Atom, Substituents, and Solvent. *ChemPhysChem* **2018**, *19*, 1315-1330.

17.   (a) Lower, S. K. and El-Sayed, M.A. The Triplet State and Molecular Electronic Processes in Organic Molecules. *Chem. Rev.* **1966**, *66*, 199-241. (b) Marian, C.M. Spin-orbit coupling and intersystem crossing in molecules. *WIREs Comput. Mol. Sci.* **2012**, *2*, 187-203.

18. Key select examples: (a) Mukherjee, S. and Thilagar P., Boron clusters in luminescent materials. *Chem. Commun.* **2016**, *52*, 1070-1093. (b) Wu, X.; Guo, J.; Quan, Y.; Jia, W.; Jia, D.; Chen, Y.; Xie, Z. Cage carbon-substitute does matter for aggregation-induced emission features

of *o*-carborane-functionalized anthracene triads. *J. Mater. Chem. C*, **2018**, *6*, 4140-4149. (c) Kim, S.; Lee, J.H.; So, H.; Kim, M.; Mun, M.S.; Hwang, H.; Hwan, M.P.; Lee, K.M. Insights into the effects of substitution position on the photophysics of mono-*o*-carborane-substituted pyrenes. *Inorg. Chem. Front.*, **2020**, *7*, 2949-2959. (d) Marsh, A.V.; Cheetham, N.J.; Little, M.; Dyson, M.; White, A.J.P.; Beavis, P.; Warriner, C.N.; Swain, A.C.; Stavrinou, P.N.; Heeney, M. Carborane-Induced Excimer Emission of Severely Twisted Bis-*o*-Carboranyl Chyrsene. *Angew. Chem. Int. Ed.*, **2018**, *57*, 10640-10645. (e) Sinha, S.; Kelemen, Z.; Hümpfner, E.; Ratera, I.; Malval, J.-P.; Jurado, J.P.; Viñas, C.; Teixidor, F.; Núñez, R.; *o*-Carborane-based fluorophores as efficient luminescent systems both as solids and as water-dispersible nanoaprticles. *Chem. Commun.*, **2022**, *58*, 4016-4019. (f) Martin, K.L.; Smith, J.N.; Young, E.R.; Carter, K.R. Synthetic Emission Tuning of Carborane-Containing Poly(dihexylfluorene)s. *Macromolecules*, **2019**, *52*, 7951-7960. (g) Li, J.; Xu, J.; Yan, L.; Lu, C.; Yan, H. A "flexible" carborane-cored luminogen: variable emission behaviours in aggregates. *Dalton Trans.*, **2021**, *50*, 8029-8035. (h) Ochi, J.; Tanaka, K.; Chujo, Y. Recent Progress in the Development of Solid-State Luminescent *o*-Carboranes with Stimuli Responsivity. *Angew. Chem. Int. Ed.*, **2020**, *59*, 9841-9855. (i) Zhang, K.; Shen, Y.; Yang, X.; Liu, J.; Jiang, T.; Finney, N.; Spingler, B.; Duttwyler, S. Atomically Defined Monocarborane Copper(I) Acetylides with Structural and Luminescence Properties Tuned by Ligand Sterics. *Chem. Eur. J.*, **2019**, *25*, 8754-8759.

TOC:

Nuc⁻ = ⁻NHR, ⁻OR, ⁻SR

Synopsis: Nucleophilic substitution of the halogen moiety at 7-I-$B_{18}H_{21}$ cluster leading to a series of new B-N, B-O and B-S substituted clusters is reported. This work highlights several independent mechanistic pathways responsible for the B-I bond breaking events and showcases how the discovered substitution chemistry can affect the luminescent properties of the newly formed cluster products.